Journal Name

COMMUNICATION

This is a peer reviewed version of the following article: J. Mater. Chem. C, 2018, 6, 960 which has been published in final form at https://pubs.rsc.org/en/content/articlelanding/2018/tc/c7tc05318e#!divAbstract.

How does alkyl chain length modify the properties of triphenylamine-based hole transport materials? †

Kun-Han Lin, Antonio Prlj and Clémence Corminboeuf*

Received 00th January 20xx,
Accepted 00th January 20xx

DOI: 10.1039/x0xx00000x

www.rsc.org/

Hole transport materials (HTMs) possessing suitable electronic properties, fast hole transport, high hydrophobicity and good oxygen resistance are critical for realizing perovskite solar cells (PSCs) that are stable and have high-performance. Manipulating the length of alkyl chains is a widely adopted strategy that can fine tune the properties of organic materials in order to enhance their performance for various applications. Yet, a systematic exploration of the influence of chain length on those properties most relevant to highly performing HTMs in PSCs is lacking. Multiscale simulations, along with morphological analyses, uncover relationships between alkyl chain length and HTM properties that provide important insights for the optimization of future organic materials.

Introduction

Hole transport materials (HTMs) based on phenylamine are commonly used in various optoelectronic applications - organic light emitting diodes[1–4], solid-state dye sensitized solar cell[5–8] and perovskite solar cells (PSCs)[9–12] – predominately because of their good transport properties, stability, and suitable ionization potential.[13] Specifically, diphenylamine (DPA) and triphenylamine (TPA) are extensively used as building blocks in high-performance or/and dopant-free HTMs of perovskite solar cells.[13–15] Spiro-OMeTAD, the current state-of-the-art, possesses four DPA groups substituted onto two fluorene units that are connected through the carbon spiro center.[16] However, the rather poor hole mobility and high cost of Spiro-OMeTAD has prompted searches for promising dopant-free DPA- or TPA-based HTMs that lead to PSCs with high power conversion efficiency (PCE) and long-term stability.[9,10,17–22] The exploration and ultimate identification of novel HTMs for PSCs relies upon establishing relevant structure-property relationships and fulfilling several requirements:

(1) **Energy alignment:** A suitable alignment of energy levels between the perovskite and hole transport layer (HTL) is required to achieve efficient hole injection. This reduces the recombination rate and increases open circuit voltage (V_{oc}).[23,24]

(2) **Optical properties:** The absorption of light falling within the range of the solar spectrum (parasitic loss) should be minimized in order to avoid competition with the perovskite active layer.[25,26]

(3) **Hole mobility:** Promising dopant-free HTMs should possess high intrinsic hole mobility (10^{-4} to 10^{-3} $cm^2V^{-1}s^{-1}$), which facilitates hole transport and reduces recombination at the perovskite/HTL interface.[12]

(4) **Hydrophobicity:** Highly hydrophobic HTMs protect the underlying perovskite layer by slowing the invasion of moisture, which leads to better long-term device performance.[19,27–31] Hydrophobic HTMs also influence the perovskite grain growth in inverted PSCs, giving rise to a perovskite layer with large grain and long carrier diffusion length.[11,32]

(5) **Oxygen resistance:** Oxygen-induced degradation is a main source of operational instability in methylammonium lead iodide PSC.[33,34] Thus, exploiting HTL as a barrier layer against O_2 diffusion[35] is beneficial.

In general, modifying the length of alkyl chains is a widely-employed approach for tuning the properties of organic materials such as: ionization potential,[36] absorption spectrum,[37] charge transport properties,[37–41] hydrophobicity[42,43] and oxygen diffusion properties.[44–47] The relationship between chain length and each of these properties is, however, not trivial and also depends on the size (small molecule or polymer) and shape (rod-shape, star shape, butterfly-shape and etc.) of molecules as well as the phase of the material (crystal or amorphous). Our previous investigation on truxene derivatives found that transport properties

Laboratory for Computational Molecular Design, Institute of Chemical Sciences and Engineering, Ecole polytechnique fédérale de Lausanne (EPFL), CH-1015 Lausanne, Switzerland. E-mail: clemence.corminboeuf@epfl.ch

† Electronic Supplementary Information (ESI) available: See DOI: 10.1039/x0xx00000x

deteriorate when hexyl side chains were present, although hydrophobicity was increased.[48] The contrasting effects brought about by the presence of hexyl chains on these two key properties demonstrate the importance of chain length optimization for improving HTM performance. Here, we elucidate relationships between side chain length and overall HTM performance using our previously established computational protocol.[48]

We selected tris[4-(9,9-dialkylfluoren-2-yl)phenyl]amine (TPAF-R), which consists of three dialkyl-substituted fluorene moieties attached to a TPA core (Figure 1), as a model system because of its suitable ionization potential (IP; 5.2 eV) and adequate hole mobility (10^{-4} $cm^2V^{-1}s^{-1}$ for the butyl substituted case).[49] Five TPAF derivatives with different chain lengths for the dialkyl component [ethyl (TPAF-E), butyl (TPAF-B), hexyl (TPAF-H), octyl (TPAF-O), and decyl (TPAF-D)] were tested by first examining the ionization potential and absorption spectra. This is followed by combining the investigation of fundamental transport quantities with a morphological analysis of amorphous HTMs. Finally, hydrophobicity and oxygen resistance are evaluated. Computational details can be found in the Supporting Information (SI).

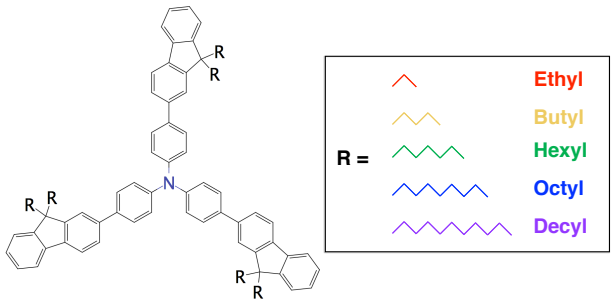

Figure 1 The TPA based molecule (TPAF-R) considered in this work.

Results and discussion

Ionization Potentials and Absorption Spectra. For TPAF-R molecules, it has been experimentally shown that alkyl chain length (ethyl, butyl and hexyl groups) only negligibly affects electronic properties such as ionization potentials (IP) and absorption spectra.[49] Our computations reproduce this finding and show minimal variation with respect to chain length (see Table S1). The IP and absorption spectra trends extracted for TPAF-R molecules stand in stark contrast to substituted truxene cores, which show pronounced differences upon elongation of aliphatic groups attached to the core.[48] The observed differences can be traced to the location of the substitution sites: in truxene, significant structural distortion occurs that disrupts the π-conjugated truxene cores, an influence, which is negligible in TPAF-R molecules. Thus, by choosing a proper substitution site, it is possible to retain the electronic and optical properties of the core, while fine-tuning other properties of interest.

Hole Mobility. Hole mobility is a critically important property that is required for promising HTMs in high performance PSCs. Here, the hole transport process is described by the hopping model, where the hopping rates between two sites are computed using non-adiabatic semi-classical Marcus charge-transfer theory. The high-temperature limit of the hopping rate between different sites is defined as:

$$\omega_{ij} = \frac{J_{ij}^2}{\hbar}\sqrt{\frac{\pi}{\lambda k_B T}}\exp\left[-\frac{(\Delta E_{ij}-\lambda)^2}{4\lambda k_B T}\right] \quad (1)$$

where T is temperature, J_{ij} is the transfer integral between i and j site, ΔE_{ij} is the site energy difference $E_i - E_j$ and λ is the reorganization energy. Analyzing disorders present in a material is essential to uncover the influence of chain length on transport properties. On one hand, *dynamic disorder,* which arises from atomic thermal fluctuations and is time-dependent, leads to a time variation of the transfer integrals and site energies. On the other hand, *static disorder* (time-independent), which originates in deviations from the perfect crystalline phase, causes the spreading of site energy values (energetic static disorder) and transfer integrals (positional static disorder).[50] Both dynamic and static disorders can dramatically reduce hole mobility of an amorphous HTM (scheme S1).[50]

The dynamic disorder of the square of the transfer integrals (J^2) is described by the coefficient of variation (C_{J^2}), as defined in the supplementary materials [Figure 2(a)]. Varying the length of the alkyl chains produces similar C_{J^2} values (within the error bars), principally because the transfer integrals are often dominated by atomic fluctuations of the π-conjugated moieties (TPA and fluorene) that are unaffected by varying the chain length. The comparable fluctuating behavior of the TPA and fluorene cores is seen by their invariant root mean square fluctuations (RMSF) [black for TPA and red for fluorene, Figure 2(b)]. Likewise, the dynamic energetic disorder, given by the standard deviation of site energy difference with time (σ_D), are also roughly similar when the error bars are considered for the different TPAF-R derivatives [Figure 2(c)]. This behavior is expected considering that the computation of site energies is dominated by electrostatic contributions involving the π-conjugated cores (see supplementary information).

In all cases, the positional static disorder dominates dynamic disorder for the transfer integrals. Therefore, the trend

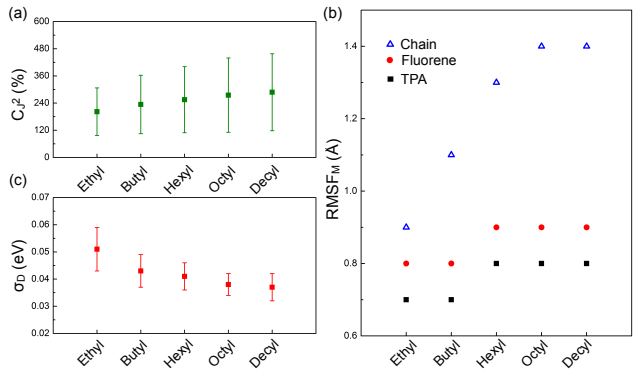

Figure 2. (a) C_{J^2}, (b) $RMSF_M$ (RSMF of a given molecular building block, *i.e.*, alkyl chains, fluorene or TPA and (c) dynamic energetic disorder of the TPAF-R derivatives.

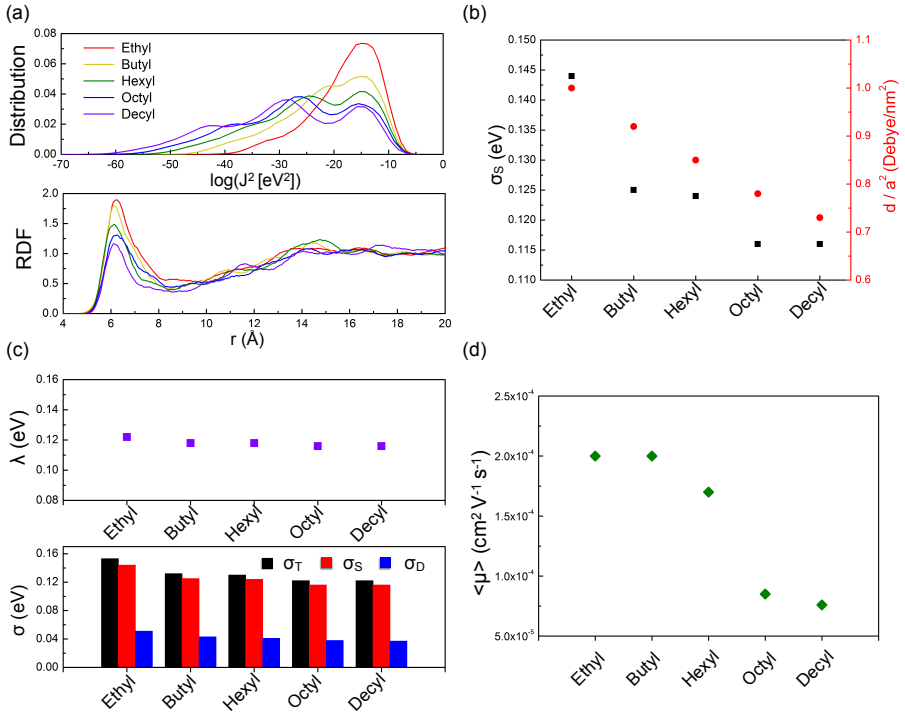

Figure 3 (a) (above) Transfer integral square distribution and (below) radial distribution function between central amine atoms, (b) static energetic disorder σ_S (black squares) and d/a^2 (red circles) and, (c) reorganization energy and energetic disorders [dynamic, static and total] and (d) hole mobility of TPAF-R molecules with different alkyl chain lengths.

associated with positional static disorder can be approximated by evaluating the total disorder of J^2 (see SI). Longer chains exhibit a broader distribution that extends into the low J^2 region (left-shifted) and lower populations in the high J^2 region [Figure 3(a)], relative to their short chain counterparts. Examination of the radial distribution functions (RDF) reveals the origin of the distinct J^2 distributions between the nitrogen atoms (amines) that characterize the morphologies of TPAF-R. The first peak, located at ~6Å, is higher for shorter chain lengths. Elongation of the aliphatic side chains inhibits close contact between the amine groups located at the center of each molecule, which causes a reduction in the first nearest neighbor (FNN) population. In turn, the smaller FNN results in a population decline in the high transfer integral region of TPAF-R for the lengthier alkyl chains. The energetic static disorder (σ_S), determined using Bredas's method,[50] is much higher than its dynamic counterpart [Figure 3(b)(c)] dropping from 0.144 eV to 0.116 eV with increasing chain length. The decline in energetic static disorder may arise from the considerable expansion in volume that accompanies longer chains (*vide infra*), as rationalized by the correlated Gaussian disorder model.[51]

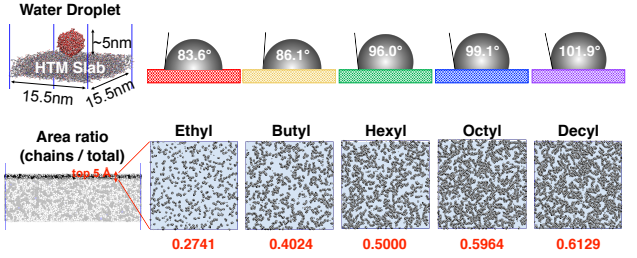

Figure 4. (above) Simulation cell and water contact angles; (bottom) the area ratio of alkyl chains to whole square area for TPAFL with different chain lengths. The VDW radii of carbon and hydrogen taken from previous work by Bondi[52] and Rowland et al.[53], respectively.

Taken together, high transfer integrals, low reorganization energy, and small energetic disorder lead to high hopping rates (Equation 1) and large hole mobility. In order to decipher how chain length affects this key property, we examined each of the fundamental transport quantities individually. Interestingly, the reorganization energies are nearly the same in all case [Figure 3(c)], whereas increasing the chain length causes a corresponding decrease in the transfer integrals [Figure 3(a)] and energetic disorder. Because of these subtle balances, TPAF-E and TPAF-B are characterized by similar hole mobilities (2.0×10^{-4} $cm^2V^{-1}s^{-1}$), as shown in Figure 3(d). Traversing the series from butyl to decyl shows hole mobility reduced from 2.0×10^{-4} to 7.6×10^{-5} $cm^2V^{-1}s^{-1}$ which is dominated by the transfer integrals [Figure 3(a)]. Note that our computed hole mobility for TPAF-B agrees well with experiment (1×10^{-4} $cm^2V^{-1}s^{-1}$),[49] which further validates our computational approach.

In order to maximize long-term performance in perovskite solar cell, it is crucial to eliminate any sources of instability (*e.g.*, H_2O and O_2) present within the device. Water invasion can be mitigated through incorporation of hydrophobic HTMs into the PSCs. The hydrophobicity of any HTM can be evaluated by determining the *water contact angle* (WCA) schematically shown in Figure 4. Longer alkyl groups, which are strongly hydrophobic, lead to higher WCAs, which rise from 83.6° (for ethyl) to 101.9° (for decyl). Influence of the chain length was gauged by computing the ratio of the area occupied by the alkyl

chains within 5 Å of the surface layer to the total square area. No aggregation of the alkyl moieties occurs, as they appear homogeneously distributed on the surface. Increasing the length of the aliphatic groups also results in greater surface coverage, which correlates well with larger computed water contact angles for the longest alkyl moieties tested. However, the increase in both WCA and area ratio appears to be nearing a plateau between the octyl to decyl groups, which implies that only marginal improvements in hydrophobicity are expected by further increasing the length of the alkyl chains. Also note that further lengthening of the alkyl moieties could modify the packing behavior of the molecules, potentially leading to a reduction in the WCA.[42,43]

The degree of O_2 resistance of an HTM can be assessed by its O_2 diffusion coefficient. In principle, the increasing free volume associated with longer chain lengths implies that O_2 should diffuse more freely in TPAF-R molecules appended with lengthy aliphatic groups [Figure 5(a)]. In reality, however, our results indicate that O_2 diffusion behavior is much more sophisticated [Figure 5(a)]. The diffusion constants decrease when moving from ethyl to hexyl, increase from hexyl to octyl, and then decrease again between octyl to decyl, which seems quite puzzling. Indeed, while longer alkyl chains provide larger free volumes, their enhanced flexibility [Figure 2(b)] can produce traps and barriers that ultimately retard diffusion, as seen by computed root mean square displacement (RMSD) for O_2 trajectories (Figures S5-S14). From these RMSD plots, O_2 diffusion behavior can be characterized as either trapped or trap-free, as shown in Figure 5(b). Due to opposing trends in free volume and flexibility, O_2 is statistically more likely to be trapped in TPAF-H (Figure S9 and S10). In addition, assuming a trap-free pattern, short alkyl groups (ethyl and butyl) tend to have larger RMSDs at the end of their trajectories compared to lengthy alkyl group (hexyl, octyl and decyl), which implies a larger O_2 diffusion barrier for the long chain cases. Since the free volume is larger for longer chain TPAF molecules, a possible origin for the higher diffusion barrier is that the alkyl chains physically obstruct O_2 molecules from diffusing. Practically speaking, tuning the length of the alkyl chains in TPAF molecules can reduce O_2 diffusion constants by up to 50% (ethyl vs. hexyl), indicating that chain length engineering can be used to improve the resistance of HTMs to O_2 ingress.

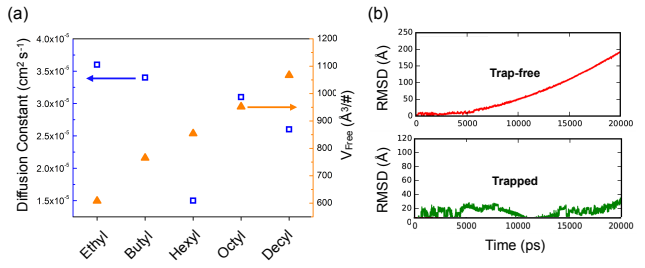

Figure 5 (a) Diffusion constant and free volume [in amorphous matrix; volume per molecule] for each case and (b) characteristic of RMSD for trap-free (red line) and trapped (green line) case.

Conclusions

In summary, we probed different properties of TPAF-R molecules in order to uncover the influence brought about by tuning the length of the alkyl chains that strongly influence HTM performance. Overall, modifying the chain length negligibly affects electronic properties but does decrease hole mobility. The degree of hydrophobicity can also be enhanced through the incorporation of longer aliphatic groups into the TPAF molecules, which remain homogeneously distributed on the surface. Concerning oxygen diffusion, the longer alkyl chains introduce more free volume which generally permits oxygen to move more freely although these groups also can serve as barriers and traps to retard oxygen diffusion. Our results show that the O_2 diffusion constant can be cut by half by finely tuning the length of the alkyl chains. Considering a holistic picture including each of the properties, TPAF-H appears to be the most promising HTM due to its highest oxygen resistance, relatively high hole mobility and water contact angle. Further elongation of the alkyl chains beyond six carbon atoms results in marginal improvement in hydrophobicity, but significant deterioration in hole mobility and oxygen resistance. In contrast, shorter chains provide slightly ameliorated hole mobility, but worse hydrophobicity as well as high oxygen diffusivity. Although the optimal chain length may be different for other amorphous HTMs, the general trends regarding chain length dependence and the rationalization from a molecular viewpoint utilized here will be beneficial for future rational designs. Moreover, this computational protocol can easily be adopted for computationally-guided design, which should increase the discovery pace of new HTMs. It should be noted that the conclusion we reach here are based on alkyl chains with even number of C and we are aware that odd-even effect of alkyl substituents can be crucial for some organic systems.[54] We will investigate this effect in the future.

Conflicts of interest

There are no conflicts to declare.

Acknowledgements

The authors thank the European Research Council (ERC Grant 306528, COMPOREL) for financial support.

References

1 M. Kimura, S. Kuwano, Y. Sawaki, H. Fujikawa, K. Noda, Y. Taga and K. Takagi, *J. Mater. Chem.*, 2005, **15**, 2393.

2 M. Aonuma, T. Oyamada, H. Sasabe, T. Miki and C. Adachi, *Appl. Phys. Lett.*, 2007, **90**, 183503.

3 Q. X. Tong, S. L. Lai, M. Y. Chan, K. H. Lai, J. X. Tang, H. L. Kwong, C. S. Lee and S. T. Lee, *Chem. Mater.*, 2007, **19**, 5851–5855.

4 Z. Jiang, T. Ye, C. Yang, D. Yang, M. Zhu, C. Zhong, J. Qin and D. Ma, *Chem. Mater.*, 2011, **23**, 771–777.

5 M. Thelakkat, *Macromol. Mater. Eng.*, 2002, **287**, 442.

6 T. Leijtens, I.-K. Ding, T. Giovenzana, J. T. Bloking, M. D. McGehee and A. Sellinger, *ACS Nano*, 2012, **6**, 1455–1462.

7 M. Planells, A. Abate, D. J. Hollman, S. D. Stranks, V. Bharti, J. Gaur, D. Mohanty, S. Chand, H. J. Snaith and N. Robertson, *J. Mater. Chem. A*, 2013, **1**, 6949–6960.

8 B. Xu, E. Sheibani, P. Liu, J. Zhang, H. Tian, N. Vlachopoulos, G. Boschloo, L. Kloo, A. Hagfeldt and L. Sun, *Adv. Mater.*, 2014, **26**, 6629–6634.

9 X. Zhao, F. Zhang, C. Yi, D. Bi, X. Bi, P. Wei, J. Luo, X. Liu, S. Wang, X. Li, S. M. Zakeeruddin and M. Grätzel, *J. Mater. Chem. A*, 2016, **4**, 16330–16334.

10 F. Zhang, C. Yi, P. Wei, X. Bi, J. Luo, G. Jacopin, S. Wang, X. Li, Y. Xiao, S. M. Zakeeruddin and M. Grätzel, *Adv. Energy Mater.*, 2016, **6**, 1600401.

11 C. Huang, W. Fu, C. Z. Li, Z. Zhang, W. Qiu, M. Shi, P. Heremans, A. K. Y. Jen and H. Chen, *J. Am. Chem. Soc.*, 2016, **138**, 2528–2531.

12 L. Calió, S. Kazim, M. Grätzel and S. Ahmad, *Angew. Chemie Int. Ed.*, 2016, **55**, 14522–14545.

13 P. Agarwala and D. Kabra, *J. Mater. Chem. A*, 2017, **5**, 1348–1373.

14 W.-J. Chi, Q.-S. Li and Z.-S. Li, *Nanoscale*, 2016, **8**, 6146–6154.

15 Z. Zhang, W. Hu, J. Cui, R. He, W. Shen and M. Li, *Phys. Chem. Chem. Phys.*, 2017, **19**, 24574–24582.

16 H.-S. Kim, C.-R. Lee, J.-H. Im, K.-B. Lee, T. Moehl, A. Marchioro, S.-J. Moon, R. Humphry-Baker, J.-H. Yum, J. E. Moser, M. Grätzel and N.-G. Park, *Sci. Rep.*, 2012, **2**, 591.

17 F. Zhang, X. Liu, C. Yi, D. Bi, J. Luo, S. Wang, X. Li, Y. Xiao, S. M. Zakeeruddin and M. Grätzel, *ChemSusChem*, 2016, **9**, 2578–2585.

18 Y.-K. Wang, Z.-C. Yuan, G.-Z. Shi, Y.-X. Li, Q. Li, F. Hui, B.-Q. Sun, Z.-Q. Jiang and L.-S. Liao, *Adv. Funct. Mater.*, 2016, **26**, 1375–1381.

19 F. Zhang, X. Zhao, C. Yi, D. Bi, X. Bi, P. Wei, X. Liu, S. Wang, X. Li, S. M. Zakeeruddin and M. Grätzel, *Dye. Pigment.*, 2017, **136**, 273–277.

20 F. Wu, B. Wang, R. Wang, Y. Shan, D. Liu, Y. K. Wong, T. Chen and L. Zhu, *RSC Adv.*, 2016, **6**, 69365–69369.

21 T. Malinauskas, D. Tomkute-Luksiene, R. Sens, M. Daskeviciene, R. Send, H. Wonneberger, V. Jankauskas, I. Bruder and V. Getautis, *ACS Appl. Mater. Interfaces*, 2015, **7**, 11107–11116.

22 D. Tomkute-Luksiene, M. Daskeviciene, T. Malinauskas, V. Jankauskas, R. Degutyte, R. Send, N. G. Pschirer, H. Wonneberger, I. Bruder and V. Getautis, *RSC Adv.*, 2016, **6**, 60587–60594.

23 S. Ryu, J. H. Noh, N. J. Jeon, Y. C. Kim, W. S. Yang, J. Seo and S. Il Seok, *Energy Environ. Sci.*, 2014, **7**, 2614–2618.

24 M. L. Petrus, T. Bein, T. J. Dingemans and P. Docampo, *J. Mater. Chem. A*, 2015, **3**, 12159–12162.

25 A. Savva, I. Burgués-Ceballos and S. A. Choulis, *Adv. Energy Mater.*, 2016, **6**, 1600285.

26 Y. Jiang, I. Almansouri, S. Huang, T. Young, Y. Li, Y. Peng, Q. Hou, L. Spiccia, U. Bach, Y.-B. Cheng, M. Green and A. Ho-Baillie, *J. Mater. Chem. C*, 2016, **4**, 5679–5689.

27 G.-W. Kim, G. Kang, J. Kim, G. Y. Lee, H. Il Kim, L. Pyeon, J. Lee and T. Park, *Energy Environ. Sci.*, 2016, **9**, 2326–2333.

28 T. Leijtens, T. Giovenzana, S. N. Habisreutinger, J. S. Tinkham, N. K. Noel, B. A. Kamino, G. Sadoughi, A. Sellinger and H. J. Snaith, *ACS Appl. Mater. Interfaces*, 2016, **8**, 5981–5989.

29 L. Zheng, Y.-H. Chung, Y. Ma, L. Zhang, L. Xiao, Z. Chen, S. Wang, B. Qu and Q. Gong, *Chem. Commun.*, 2014, **50**, 11196–11199.

30 Y. S. Kwon, J. Lim, H.-J. Yun, Y.-H. Kim and T. Park, *Energy Environ. Sci.*, 2014, **7**, 1454–1460.

31 P. Y. Su, Y. F. Chen, J. M. Liu, L. M. Xiao, D. Bin Kuang, M. Mayor and C. Y. Su, *Electrochim. Acta*, 2016, **209**, 529–540.

32 C. Bi, Q. Wang, Y. Shao, Y. Yuan, Z. Xiao and J. Huang, *Nat. Commun.*, 2015, **6**, 7747.

33 D. Bryant, N. Aristidou, S. Pont, I. Sanchez-Molina, T. Chotchunangatchaval, S. Wheeler, J. R. Durrant and S. A. Haque, *Energy Environ. Sci.*, 2016, **9**, 1655–1660.

34 N. Aristidou, I. Sanchez-Molina, T. Chotchuangchutchaval, M. Brown, L. Martinez, T. Rath and S. A. Haque, *Angew. Chemie - Int. Ed.*, 2015, **54**, 8208–8212.

35 J. You, L. Meng, T.-B. Song, T.-F. Guo, Y. (Michael) Yang, W.-H. Chang, Z. Hong, H. Chen, H. Zhou, Q. Chen, Y. Liu, N. De Marco and Y. Yang, *Nat. Nanotechnol.*, 2015, **11**, 75–81.

36 B. Friedel, C. R. McNeill and N. C. Greenham, *Chem. Mater.*, 2010, **22**, 3389–3398.

37 A. Cadisa, W. D. Oosterbaan, K. Vandewal, J. C. Bolsée, S. Bertho, J. D'Haen, L. Lutsen, D. Vanderzande and J. V. Manca, *Adv. Funct. Mater.*, 2009, **19**, 3300–3306.

38 A. Babel and S. A. Jenekhe, *Synth. Met.*, 2005, **148**, 169–173.

39 J. Min, Y. N. Luponosov, A. Gerl, M. S. Polinskaya, S. M. Peregudova, P. V. Dmitryakov, A. V. Bakirov, M. A. Shcherbina, S. N. Chvalun, S. Grigorian, N. Kaush-Busies, S. A. Ponomarenko, T. Ameri and C. J. Brabec, *Adv. Energy Mater.*, 2014, **4**, 1–10.

40 E. 0 Arikainen, N. Boden, R. J. Bushby, J. Clements, B. Movaghar and A. Wood, *J. Mater. Chem*, 1995, **5**, 2161–2165.

41 I. Osaka, R. Zhang, G. Sauvé, D.-M. Smilgies, T. Kowalewski and R. D. McCullough, *J. Am. Chem. Soc.*, 2009, **131**, 2521–2529.

42 T. Ishizaki, N. Saito, L. SunHyung, K. Ishida and O. Takai, *Langmuir*, 2006, **22**, 9962–9966.

43 M. Okouchi, Y. Yamaji and K. Yamauchi, *Macromolecules*, 2006, **39**, 1156–1159.

44 I. Pinnau, A. Morisato and Z. He, *Macromolecules*, 2004, **37**, 2823–2828.

45 G. Pu, M. L. Longo and M. a Borden, *J. Am. Chem. Soc.*, 2005, **127**, 6524–6525.

46 S. G. Charati and S. a. Stern, *Macromolecules*, 1998, **31**, 5529–5535.

47 B. A. Kowert and N. C. Dang, *J. Phys. Chem. A*, 1999, **103**, 779–781.

48 K.-H. Lin, A. Prlj and C. Corminboeuf, *J. Phys. Chem. C*, 2017, **121**, 21729–21739.

49 M. Sonntag, K. Kreger, D. Hanft, P. Strohriegl, S. Setayesh and D. de Leeuw, *Chem. Mater.*, 2005, **17**, 3031–3039.

50 N. R. Tummala, Z. Zheng, S. G. Aziz, V. Coropceanu and J.-L. Brédas, *J. Phys. Chem. Lett.*, 2015, **6**, 3657–3662.

51 S. V Novikov, D. H. Dunlap, V. M. Kenkre, P. E. Parris and a V Vannikov, *Phys. Rev. Lett.*, 1998, **81**, 4472–4475.

52 A. Bondi, *J. Phys. Chem.*, 1964, **68**, 441–451.

53 R. S. Rowland and R. Taylor, *J. Phys. Chem.*, 1996, **100**, 7384–7391.

54 T. Lei, J.-Y. Wang and J. Pei, *Chem. Mater.*, 2014, **26**, 594–603.

